JOURNAL OF MATERIALS SCIENCE 32 (1997) 1049–1053

Effects of quenching treatment on the structure and electrical property in doped V_2O_3 system

W. CHEN, Q. XU, W. Q. CUI
Department of Materials Science, Wuhan University of Technology, Wuhan 430070 Hubei People's Republic of China

The effects of quenching treatment are examined in terms of the phase present, microstructure and electrical properties for doped V_2O_3 system, in this paper. The results indicate that the specimens transform to the PM phase and show microcracks in the structure after quenching. The room temperature (RT) resistivities become low and the resistivity ratios increase remarkably. There are optimum values for the RT resisitivity and resisitivity ratio under a certain quenching time. The electrical properties of quenched specimens containing Fe metal phase become stable after subsequent thermal cycles.

1. Introduction

Metal-doped vanadium sesquioxide $(V_{1-x}M_x)_2O_3$ exhibits a variety of metal–insulator transformations as a function of temperature, pressure and doping concentration, x [1]. The PM–PI transformation at high temperature provides the potential for doped V_2O_3 to be used as a functional positive temperature coefficient (PTC) material [2]. Work on single crystals of the material shows that there is an increase in resistivity of about two orders of magnitude over a temperature range of 15 K [3], a volume increase of 1.2% and a shear strain of 0.8% although the crystal symmetry is unchanged [1]. The transition temperature can vary with doped oxides and dopant concentrations. This transformation shows a hysteresis of about 50 K between heating and cooling. On the other hand, electrical properties, especially the switching action of doped V_2O_3 ceramic, are strongly influenced by internal stress generated during its manufacture [4]. To achieve the optimum performance and reliability of the PTC thermistor, some special treatments are adopted in the ceramic processing [5].

In this paper, the technology of quenching in liquid nitrogen is used for doped V_2O_3 ceramics. With modern measuring methods, it is shown that the electrical properties and structure are affected by the quenching treatment. In the meantime, the optimum parameters for the treatment are determined.

2. Experimental details

The specimens were prepared from V_2O_5, Cr_2O_3, Al_2O_3, Fe_2O_3, SnO_2 and CuO (99.99%). The V_2O_5 powder was reduced to V_2O_3 in an environment of H_2 gas at temperature from 600 to 900 °C. The V_2O_3 powder was mixed with the dopant oxides at the concentrations listed in Table I. Mixing was performed in agate vessels; pellets of about 1.5 g were pressed at a pressure of 900 MPa using polyvinyl acetate as a binder. The pellets were then sintered at 1450–1500 °C in H_2 for 4 h. All reduction and sintering steps were performed in alumina boats. On the other hand, all specimens were quenched in liquid nitrogen; with B_6 being quenched for different times. The densities of the specimens were measured gravimetrically; the results are also shown in Table I.

X-ray diffraction (XRD) was used to determine the phases present in the sintered pellets and the quenched pellets. The pellets were examined by scanning electron microscopy (SEM) to study the grain shape, size, pore size and microcracks. The back scattering electron image of SEM was used to determine the distribution of the metal phase in the specimens.

The electrical measurements were undertaken by using a four-point probe perpendicular to the pressing direction of the pellets. The voltage was measured with a potentiometer with a resolution of 0.02 mV. The current was varied from 1 to 180 mA giving a range of resistance measurements from 1×10^{-4} to $1 \times 10^{+4}\,\Omega$. Copper leads were clamped to both surfaces of the specimen with special electrodes. The clamp ensured that the connection could be maintained through the large strains associated with the phase transformation.

3. Results and discussion

3.1. Phase present

Compared with the standard XRD pattern of V_2O_3, the XRD pattern of B_1 is shown to be pure V_2O_3 crystal phase. The XRD patterns of other specimens are similar to that of B_1, except for trace differences between the d values or relative intensity. It has been proved that Cr_2O_3 and Al_2O_3 dissolve in the V_2O_3 lattice [5, 6]. In addition, the XRD patterns of B_6, B_8, B_9, B_{11} show some small diffraction peaks of a

0022–2461

TABLE I The composition and density of specimens with various dopant concentrations

Specimen	Composition	Density (g cm^{-3})	Relative density (%)
B_1	V_2O_3	4.66	92.4
B_2	$(V_{0.9950}Cr_{0.0050})_2O_3$	4.76	94.5
B_3	$(V_{0.9950}Cr_{0.0025}Al_{0.0025})_2O_3$	4.81	95.5
B_6	$(V_{0.9950}Cr_{0.0050})_2O_3$ + 10 wt % Fe	5.20	98.0
B_8	$(V_{0.9950}Cr_{0.0025}Al_{0.0025})_2O_3$ + 10 wt % Sn	4.95	97.0
B_9	$(V_{0.9950}Cr_{0.0050})_2O_3$ + 10 wt % Cu	5.25	96.8
B_{11}	$(V_{0.9950}Cr_{0.0050})_2O_3$ + 20 wt % Fe	5.43	97.0

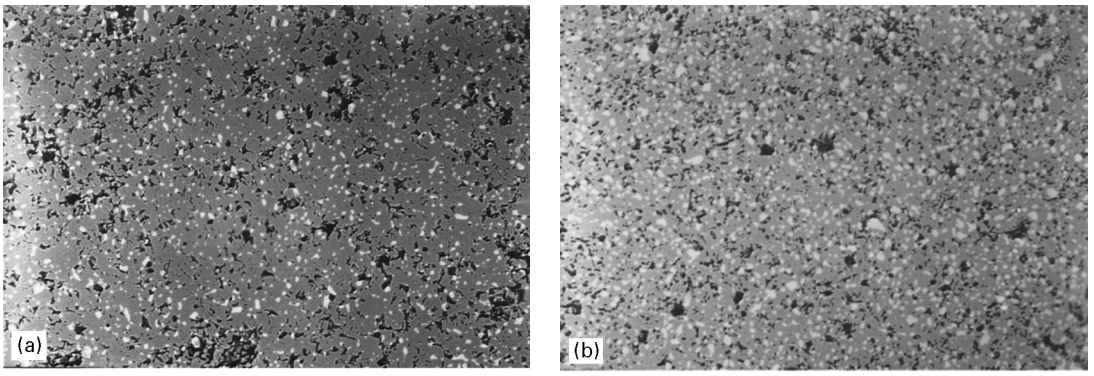

Figure 1 The back-scattering electron images of (a) B_6 and (b) B_{11}.

TABLE II The result of XRD for specimens

Specimen	a (nm)	c (nm)	c/a	Volume	Phase	Phase content (%)
B_1	4.949	13.975	2.84	296.4	PM	100
B_2	4.989	13.869	2.78	299.0	PI	75
	4.973	13.961	2.81	298.0	PM	25
B_3	4.990	13.840	2.77	298.5	PI	74
	4.956	13.976	2.82	297.3	PM	26
B_6	4.943	13.957	2.82	295.3	PM	90
B_8	4.954	13.942	2.81	296.3	PM	72
	4.974	13.878	2.79	297.4	PI	28
B_9	4.954	13.952	2.82	296.5	PM	88
	4.976	13.868	2.79	297.5	PI	12
B_{11}	4.957	13.929	2.81	296.4	PM	92
B_2(CL)*	4.966	13.975	2.81	298.5	PM	100
B_8(CL)*	4.958	13.932	2.81	296.6	PM	100
B_{11}(CL)*	4.948	13.993	2.83	296.7	PM	100

*CL: diffraction data taken after quenching.

metal phase. It is thought that SnO_2, CuO and Fe_2O_3 are reduced into Sn, Cu and Fe in H_2 gas, respectively. The metal phases are regarded as the dispersed second-phase particles existing in the structure. The back-scattering electron images of B_6 and B_{11} shown in Fig. 1 indicate that Fe is homogeneously dispersed in the matrix of doped V_2O_3 ceramic. The XRD patterns of the quenched specimens also show a slight change in the d values or intensity compared with the same specimens without quenching.

To understand better the change of phase present, the lattice constants were calculated. For simplicity, the rhombohedral phases were indexed on a hexagonal lattice, and a least squares determination of the a and c hexagonal lattice parameters determined by using the diffraction peaks of (0 1 2), (1 0 4), (1 1 0), (1 1 3), (0 2 4) and (1 1 6). The results of XRD are shown in Table II. The PM and PI phases can be distinguished by the c/a ratio (hexagonal) [1]. The absolute values of c and a are not accurately calibrated, and the volumes can not be compared from specimen to specimen. The measured unit cell volumes of the PM and PI phases in any one specimen are given for comparison. The specimens contain both the PM and PI phases. The relative contents of the phase can be estimated from the relative peak intensity proportions of the PM and PI phases in the same specimen. The results show that the PI phase in the specimens is transformed to the PM phase, and a volume decrease exists after quenching. So the quenched specimens only contain the PM phase.

3.2. Microstructure

When cooled down to room temperature from high temperature, thermal stress must remain in

the sintered specimens. The thermal stress in specimens is relaxed after quenching. There is no doubt that the thermal stress relaxation and the volume decrease caused by the PI–PM transformation must affect the microstructure of the specimens. Figs 2 and 3 are the SEM photographs of B_2, B_{11} before and after quenching, respectively. It is observed from Fig. 2a that the grains grow well, the grain rims are clear and the grains are closely linked together. The quenched specimen shows a few microcracks which are along grain boundaries and through grains (as shown in Fig. 2b). The grain rims shown in Fig. 3a are less clear than those in Fig. 2a. This can be explained by the Fe reduced by H_2 gas soaking the grain surfaces at high temperature and existing in the grain boundaries when cooled down. Therefore, the grains mostly show irregular shapes. B_{11} contains a small amount of PI phase and the volume decrease caused by the PI–PM transformation is very small. Furthermore, the Fe has better ductility and can partly buffer the volume change and the thermal stress when quenching. Fig. 3b shows only a few microcracks in the grains. The microcrack size is much smaller and the number is much fewer than that seen in Fig. 2b. It is proved that the dispersed metal phase is very advantageous to improve the microstructural stability of the quenched specimens.

3.3. The electrical properties

The electrical properties of the specimens are associated not only with the doping element and concentrations but also the phase present and microcracks. This is to say that the electrical properties are influenced by the quenching treatment. The measured electrical properties are shown in Table III. The RT resistivities of quenched specimens are all lower than that of the same specimens without quenching. It is explained that the PI phase in specimens is transformed to the PM phase and the resistivities become low. The RT character of the material will show this change before and after quenching. Because the PTC effect originates from the PM–PI transformation over room temperature and is restrained by the thermal stress remaining in the specimens, B_2 and B_3 do not show a PTC effect. However, the specimens containing metal phases have the most partial PM phase, and the stress will be partly relaxed by the ductile metal phases. They show a PTC effect over room temperature. After quenching, the PI phase is transformed to the PM phase, and thermal stress is efficiently relaxed. In the meantime, the microcracks can provide the space for the volume increase caused by the PM–PI transformation in the specimens without a metal phase. Therefore, the quenched B_2 and B_3 show an obvious PTC effect. Even though the specimens containing metal phase produce few microcracks, the metal ductility will make up for the volume increase of the PM–PI transformation. The quenched specimens show a remarkable increase in the resistivity ratio compared with the same specimens without quenching. Additionally, there is the most remarkable increase for quenched B_6.

To analyse further the effect of quenching on the electrical properties, measurements were made on B_6 for different quenching times. The results are shown in

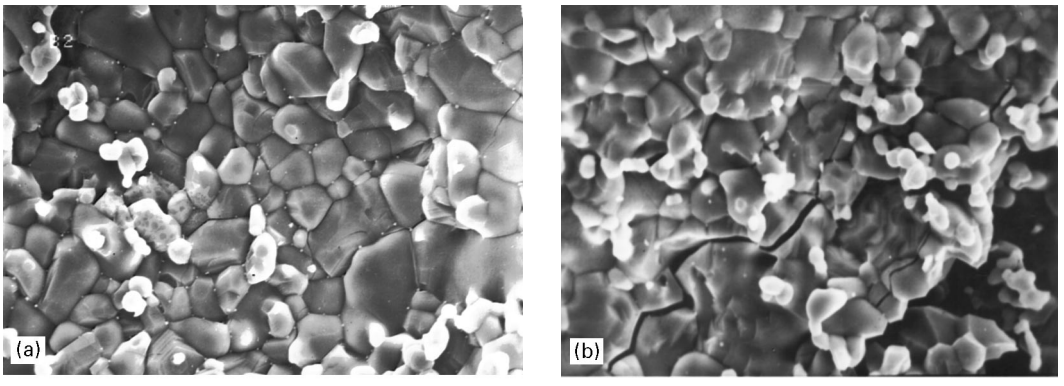

Figure 2 The SEM photograph of B_2 (a) before quenching and (b) after quenching.

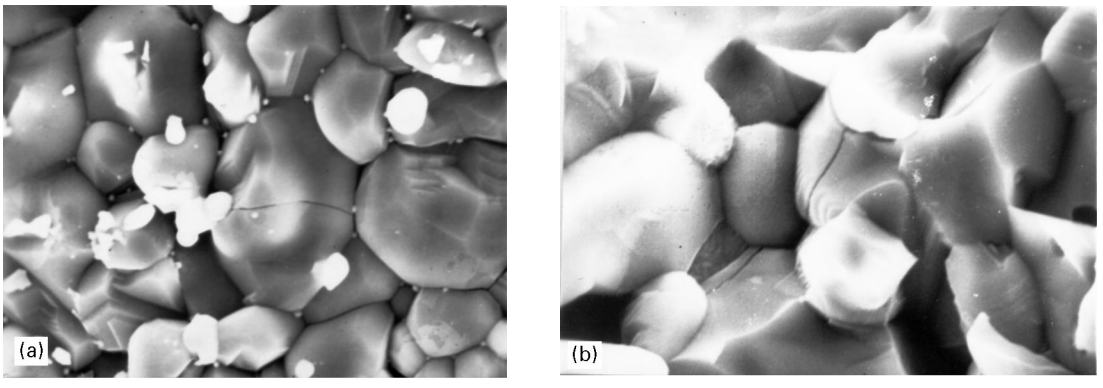

Figure 3 The SEM photograph of B_{11} (a) before quenching and (b) after quenching.

TABLE III The measured electrical properties of specimens

Specimen	RT resistance, $\rho_{20\,^\circ C}$(Ω cm)		Resistance ratio, $\rho_{max}/\rho_{20\,^\circ C}$		Curie temperature T_C(°C)		RT character of the material	
	ST	CL	ST	CL	ST	CL	ST	CL
B_1	9.60×10^{-3}	–	–	–	–	–	–	–
B_2	4.20×10^{-1}	1.42×10^{-2}	–	30	–	96	–	PTC
B_3	1.97×10^{-1}	5.81×10^{-2}	–	36	–	94	–	PTC
B_6	1.76×10^{-3}	7.16×10^{-4}	46	231	116	119	PTC	PTC
B_8	1.68×10^{-2}	1.04×10^{-2}	24	48	118	123	PTC	PTC
B_9	7.21×10^{-2}	2.30×10^{-2}	19	45	108	116	PTC	PTC
B_{11}	7.68×10^{-2}	1.82×10^{-2}	22	68	104	112	PTC	PTC

The quenching time of all specimens is 30 min.
ST: data taken before quenching.
CL: data taken after quenching.

TABLE IV The electrical properties of B_6 with different quenching times

Electrical property	Time (min)					
	0	20	30	40	60	80
RT resistance, $\rho_{20\,^\circ C}$(Ω cm)	1.76×10^{-3}	9.46×10^{-4}	7.16×10^{-4}	6.60×10^{-4}	1.30×10^{-3}	5.84×10^{-3}
Resistance ratio, $\rho_{max}/\rho_{20\,^\circ C}$	46	97	231	252	66	35

TABLE V The electrical properties of B_6 quenched for 40 min with three thermal cycles

Property	First cycle		Second cycle		Third cycle	
	Heating	Cooling	Heating	Cooling	Heating	Cooling
RT resistance, $\rho_{20\,^\circ C}$(Ω cm)	6.60×10^{-4}	6.60×10^{-4}	6.60×10^{-4}	6.60×10^{-4}	6.60×10^{-4}	6.60×10^{-4}
Resistance ratio, $\rho_{max}/\rho_{20\,^\circ C}$	252	345	287	368	302	371
Curie temperature, T_C(°C)	120	78	116	84	114	85

Table IV. It is known that the lowest RT resistivity and the largest resistivity ratio is obtained under quenching for 40 min. Then, the RT resistivity will become high and the resistivity ratio will become small with increasing quenching time. This is explained by the PI phase gradually transforming to the PM phase and thermal stress gradually relaxing, and the microcracks increase in number or expand in size with quenching time. The RT resistivity and resistivity ratio reflect the phase, thermal stress and microcracks formed during processing with the optimum values for the electrical properties being obtained following quenching for 40 min. When the quenching time is more than 40 min, the microcracks further increase in number or expand in size. Though the microcracks are advantageous to the PM–PI transformation, the microcracks can be considered as an insulator phase [7]. Therefore, excessive microcracks will have a disadvantageous effect on the PTC properties. To study the stability of electrical properties for quenched specimens, the electrical properties of B_6 quenched for 40 min were measured over three cycles of heating and cooling. The data are shown in Table V. The results show that the RT resistivity is almost unchanged over three thermal cycles, the resistivity ratio of heating or cooling gradually becomes a constant and the hysteresis size becomes narrow with cycle times. It is indicated that the electrical properties are very stable for quenched specimens. Therefore, the quenching treatment may be applicable for making PTC materials of the doped V_2O_3 system.

4. Summary

1. The specimens containing part of the PI phase are transformed to the PM phase by the quenching treatment.

2. The quenched specimens without metal phase show the microcracks which are along the grain boundary and through the grain. The quenched specimens containing metal phase show only few microcracks in the grain which are smaller in size and much fewer in number than those of the specimens without metal phase.

3. The specimens containing metal phase and the quenched specimens exhibit a PTC effect. The RT resistivity becomes small and the resistivity ratio becomes large after quenching. Optimum values for the RT resistivity and the resistivity ratio under a certain quenching time were obtained.

The electrical properties of the quenched specimens containing Fe phase will gradually become stable with thermal cycling times.

References

1. D. B. MCWHAN and J. P. REMEIKA, *Phys. Rev. B.* **9** (1970) 3734.
2. R. S. PERKINS, A. RÜEGG, M. FISCHER, P. STREIT and A. MENTH, *IEEE Trans. Components, Hybrids Manuf. Technol.* **2** (1982) 225.
3. H. KUWAMOTO, J. M. HONIG and J. APPEL, *Phys. Rev. B.* **22** (1980) 2626.
4. R. S. PERKINS, A. RÜEGG and M. FISCHER, *Adv. Ceram. Addit. Interfaces Electron. Ceram.* **7** (1983) 166.
5. W. CHEN, Q. XU, W. Q. CUI, Y. Q. ZHOU, M. HONG and F. B. ZHAO, *J. Wuhan Univ. Technol.* (Chinese) **2** (1994) 18.
6. B. C. HENDIX, X. WANG, W. CHEN and W. Q. CUI, *J. Mater. Sci.: Mater. Electron.* **3** (1992) 113.
7. A. RÜEGG, R. S. PERKINS and P. STREIT, *Sci. Ceram.* **11** (1981) 559.

Received 20 November 1995
and accepted 17 September 1996